Journal of Zhejiang University-SCIENCE A (Applied Physics & Engineering) in press
www.jzus.zju.edu.cn; www.springer.com/journal/11582
E-mail: jzus_a@zju.edu.cn

Correspondence

https://doi.org/10.1631/jzus.A2400062

COM trajectory planning and disturbance-resistant control of a bipedal robot based on CP-ZMP-COM dynamics

Chunbiao GAN[1,2]✉, Zijing LI[1,2], Yimin GE[1,2], Mengyue LU[1,2]

[1]*State Key Laboratory of Fluid Power and Mechatronic Systems, School of Mechanical Engineering, Zhejiang University, Hangzhou 310058, China*
[2]*Key Laboratory of Advanced Manufacturing Technology of Zhejiang Province, School of Mechanical Engineering, Zhejiang University, Hangzhou 310058, China*

1 Introduction

To date, in model-based gait-planning methods, the dynamics of the center of mass (COM) of bipedal robots have been analyzed by establishing their Linear Inverted Pendulum Model (LIPM) or extended forms (Englsberger et al, 2015; Jones and Wang, 2018; Xie et al, 2020). With regard to model-based gait-generation methods for uphill and downhill terrain, Kuo (Kuo, 2007) simulated human gait using an inverted pendulum, which provided a circular trajectory for the COM rather than a horizontal trajectory. He found that a horizontal COM trajectory consumed more muscle energy. Massah et al (Massah et al, 2012) utilized a 3D LIPM and the concept of Zero Moment Point (ZMP). They developed a trajectory planner using the semi-elliptical motion equations of a NAO humanoid robot and simulated walking on various sloped terrains using the Webot platform.

In bipedal robot motion control based on the LIPM, the COM, ZMP, and Capture Point (CP) are crucial factors for achieving stable walking. Addressing the issue of implementing synchronized stabilization control schemes for ZMP and COM, Choi et al (Choi et al, 2007) introduced a kinematic decomposition method for the COM Jacobian matrix, including embedded desired task motion. Hof (Hof, 2008) independently introduced the CP concept, which defined the position where a bipedal robot can step on the ground to achieve complete stoppage, thereby providing a simple walking balance-control method. Building upon the CP concept, Englsberger et al. (Englsberger et al, 2011) developed a trajectory generator and feedback controller for bipedal robots. Joe and Oh (Joe and Oh, 2018) proposed an online walking-pattern-generation algorithm based on footprint adjustment, enabling bipedal robots to effectively restore walking balance after external disturbances.

In 2020, Yamamotoa et al (Yamamotoa et al, 2020) briefly surveyed the centroidal dynamics and the zero-moment point based on the LIPM and some of its variations; they reviewed many representative standing and walking control techniques based on the LIPM, and also discussed the concept of capturability. Recently, Park et al (Park et al, 2022) proposed a new stability criterion for bipedal walking systems based on the LIPM, in which the dynamic relationship between the CoM and the ZMP was dealt with. Furthermore, the adaptive-network-based fuzzy inference system (ANFIS) was combined with the double deep Q-network (DDQN) to realize a fuzzy DDQN (FDDQN), such that a bipedal robot could generate a LIPM-based gait pattern in real time. This not only allowed the bipedal robot to correct its gait pattern instantly but also improved its stability (Li THS et al, 2022).

Kajita et al ensured the simplicity and flexibility of classical gait-planning methods, borrowing the idea of "preview controllers" that optimize current

✉ Chunbiao GAN, cb_gan@zju.edu.cn
Chunbiao GAN, https://orcid.org/0000-0002-6597-5605

Received Feb. 2, 2024; Revision accepted June 5, 2024; Crosschecked

© Zhejiang University Press 2024

Unedited

decisions based on future information to optimize the inevitable foot-placement deviations in classical gait-planning methods (Kajita et al, 2014). Based on the LIPM, we propose a closed-loop feedback-control method for bipedal robot COM trajectory planning and resistance to external force disturbances based on CP-ZMP-COM dynamics. The method is based on our analysis of the COM motion trajectories in the sagittal and coronal planes.

2 COM trajectory planning based on CP-ZMP-COM dynamics

As shown in Fig. 1(a), the LIPM maintains the COM of a bipedal robot moving on a horizontal plane with a height of z_0, using a scalable, massless leg with its pivot located at the robot's ZMP. In the LIPM, the equations of motion for the robot's COM are linear and decoupled, and the dynamical analysis can be equivalently and independently used for the two components x and y of the robot. Fig. 1(b) presents the decoupled model of the three-dimensional LIPM in the x-z plane, where the position of the robot's COM is expressed as $\boldsymbol{P}_c = [x_{\mathrm{com}}, z_0]^{\mathrm{T}}$, the pivot (i.e., ZMP point) position is $\boldsymbol{P}_a = [p_x, 0]^{\mathrm{T}}$, the ground reaction force F_{t} acts through the pivot and COM, F_{v} and F_{h} are its components in the x and y directions, respectively, F_{r} is the external force acting on the COM in the x direction, and F_g is gravity. Based on Newton's theorem and the relationship $F_{\mathrm{h}} / F_{\mathrm{v}} = F_{\mathrm{r}} / F_g = (m\ddot{x}_{\mathrm{com}}) / (mg) = (x_{\mathrm{com}} - p_x) / z_0$, the dynamic model of the bipedal robot's CP-ZMP-COM can be established as follows:

$$\dot{\boldsymbol{\theta}} = \begin{bmatrix} -\omega_0 & \omega_0 \\ 0 & \omega_0 \end{bmatrix} \boldsymbol{\theta} + \begin{bmatrix} 0 \\ -\omega_0 \end{bmatrix} p_{\mathrm{x}} \tag{1}$$

in which $\omega_0 = \sqrt{g / z_0}$, $\boldsymbol{\theta} = [x_{\mathrm{com}}, \xi_x]^{\mathrm{T}}$ and $\xi_x = x_{\mathrm{com}} + \dot{x}_{\mathrm{com}} / \omega_0$ is the CP in the x-direction of the robot. The detailed derivation for Eq. (1) is presented in Data S1.

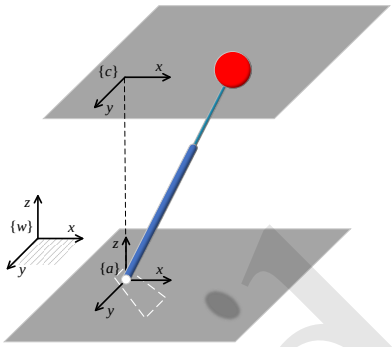

(a) Three-dimensional model

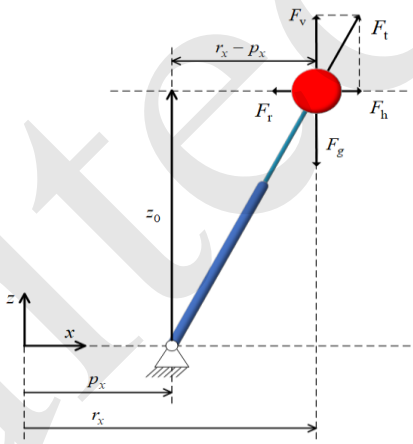

(b) Decoupled model in the x-z plane

Fig. 1 LIPM for bipedal robot.

The COM trajectory planning method for the bipedal robot was based on CP-ZMP-COM dynamics and can be briefly outlined as follows: By utilizing the ZMP-CP dynamics $\dot{\xi}_x = \omega_0 (\xi_x - p_x)$, the CP-COM dynamics $\dot{x}_{\mathrm{com}} = -\omega_0 (x_{\mathrm{com}} - \xi_x)$ automatically track the CP. By adjusting the robot's foot placement to control the COM trajectory, as represented by the ZMP-COM dynamics, the robot's COM trajectory can be planned. The kinematic relationship among ZMP, CP, and COM is shown in Fig. 2, where ξ_{e} is the expected final position of the CP; the specific steps are also listed in Data S1.

It should be noted that due to the discrepancy between the real robot dynamics and the simplified inverted pendulum dynamics (see Fig. 6 in Section 4), using this controller will result in a non-constant ZMP (see Fig. 7). However, it still ensures that the robot's ZMP remains within a feasible range for walking continuously without falling when there is no external disturbance imposed on the robot (see the screenshots shown in Fig. 7).

Unedited

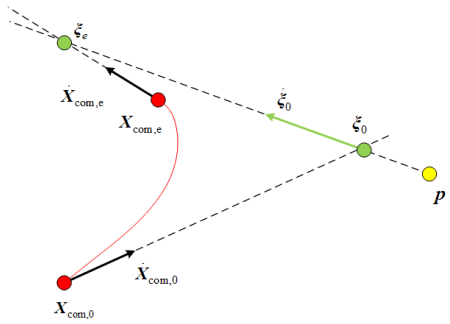

Fig. 2 Kinematic relationship among ZMP, CP, and COM. The path of COM is represented by the red curve.

3 Anti-disturbance feedback compensation control

During walking, adults exhibit a swaying motion of their COMs in the sagittal plane, resembling that of an inverted pendulum, as they dynamically adjust their step lengths. This allows for either short, quick steps or long, slow steps, while maintaining constant COM walking speed. Therefore, coordinating the foot placement of the robot in both the sagittal and coronal planes was crucial to counteracting external disturbances.

Inspired by this, further characterization of the robot's gait parameters during walking was required. As shown in Fig. 3, the LIPM was placed in the ankle joint {a} coordinate system (i.e., ZMP point, as shown in Fig. 1(a)). In ideal conditions, the undisturbed trajectory of the robot's COM serves as the nominal gait reference trajectory, based on which the gait parameters are explicitly defined to avoid confusion.

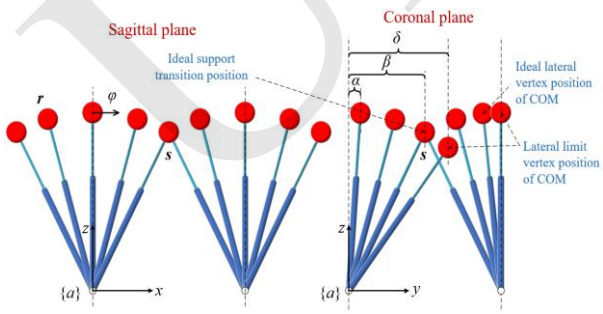

Fig. 3 Gait parameters in sagittal and coronal planes of bipedal robot during walking process.

As shown in Fig. 3, the reference trajectory of bipedal robotic walking, which switches supporting legs, takes its COM state as the ideal characteristic gait, depending solely on its walking velocity $\boldsymbol{v}$ and four additional gait parameters, α, β, δ, and φ: Parameter α represents the distance between the origin of the supporting coordinate system {a} and the COM in the y-direction (lateral) when the COM is at the coronal-plane vertex position (at which time the velocity $\dot{c}_y$ of COM in the y-direction is 0); β represents the distance in the y-direction between the COM and the supporting coordinate system when exchanging supporting feet; δ represents the distance between COM and the origin of the supporting coordinate system in the y-direction (in the sagittal plane) under the limit state of exchanging support, at which time the velocity $\dot{c}_y$ of COM in the y-direction is at its maximum of $v_y^{\max}$; and φ represents the magnitude of COM velocity in the x-direction $\dot{c}_x$ when COM is at the vertex position of the sagittal plane (at which time $v_x^{\max}$ is the maximum velocity of COM). Additionally, when the robot's COM is at the position defined by parameter α, the lateral component of the COM velocity is zero. As long as α is greater than zero, the COM will tend towards the direction of the next foothold and ensure that the support exchange position is reached within the ranges of β and δ.

Let $\boldsymbol{v} = (v_x, v_y)^{\mathrm{T}}$ denote the desired walking-velocity input vector, where each component represents the reference walking speed in the forward and lateral directions, respectively. According to the COM dynamics (Eq. (2) in Data S1), the ideal COM state during support exchange is given by $\boldsymbol{s} = (s_x, \dot{s}_x, s_y, \dot{s}_y)^{\mathrm{T}}$, where

$$s_y = \begin{cases} \lambda\zeta, & \text{if } \lambda = \operatorname{sgn}(v_y) \\ \lambda\beta, & \text{else} \end{cases} \tag{2a}$$

$$\dot{s}_y = \lambda C\sqrt{s_y^2 - \alpha^2} \tag{2b}$$

$$s_x = \frac{\varphi v_x}{C v_x^{\max}} \sinh(C\tau) \tag{2c}$$

$$\dot{s}_x = \frac{\varphi v_x}{v_x^{\max}} \cosh(C\tau) \tag{2d}$$

Unedited

In Eq. (2a), $\zeta = \beta + |v_y|(\delta - \beta)/v_y^{\max}$ denotes the lateral support-swapping position required when the robot needs lateral walking speed; in Eq. (2b), $\lambda \in \{-1,1\}$ represents the left-right sign of the assumed supporting leg; while in Eq. (2c), $\tau = \frac{1}{C}\ln\left(\frac{\zeta}{\alpha} + \sqrt{\frac{\zeta^2}{\alpha^2} - 1}\right)$ stands for the transition time of COM from the vertex to the support-swapping position, where C is the parameter reflecting the gravitational influence on the point-mass trajectory (Pratt et al, 2006). The COM state $\boldsymbol{s}$ at this ideal support-swapping position defines the goal of the controller, aiming to adjust the foothold to achieve this goal at the end of the next step.

Based on the above analysis, the specific steps for the feedback compensation control method are as follows:

Step 1 Input the initial desired walking velocity vector $\mathbf{v}_0$, and calculate the ideal COM state trajectory $\boldsymbol{s} = (s_x, \dot{s}_x, s_y, \dot{s}_y)^{\mathrm{T}}$ using COM dynamics (Eq. (2) in Data S1), then proceed to Step 2.

Step 2 Based on the actual COM state $\boldsymbol{c} = (c_x, \dot{c}_x, c_y, \dot{c}_y)^{\mathrm{T}}$ in the current support-foot coordinate system of the biped robot and the ideal COM state $\boldsymbol{s} = (s_x, \dot{s}_x, s_y, \dot{s}_y)^{\mathrm{T}}$ during support switching, calculate the following five compensation parameters, i.e., lateral ZMP compensation y_{offset}, support-switching time interval $\mathrm{d}T$, lateral step width L_y, forward ZMP compensation x_{offset}, and forward step length L_x (which are listed in Data S1), then proceed to Step 3.

Step 3 Substitute the results of Step 2 into the CP controller: $p_x = \frac{\xi_{x,d} - e^{\omega_0 \mathrm{d}T}\xi_x}{1 - e^{\omega_0 \mathrm{d}T}} = \frac{1}{1-b}\xi_{x,d} - \frac{b}{1-b}\xi_x$ (3) (Eq. (9) in Data S1); update and record the coordinates of the support leg and the ideal COM state, then proceed to Step 4.

Step 4 Based on the results recorded in Step 3, input the reference trajectories of each joint obtained from inverse kinematics calculations into the prototype servos to achieve walking control of the prototype. Update and record the coordinates of the support leg and the actual COM state of the physical prototype using joint encoders and an Inertial Measurement Unit (IMU), then proceed to Step 5.

Step 5 Compare and analyze the errors between the coordinates of the support leg and the COM state under ideal conditions, and the coordinates of the support leg and the COM state of the actual physical prototype. Return to Step 2.

The algorithm flowchart for the feedback compensation control method is given in Fig. 4.

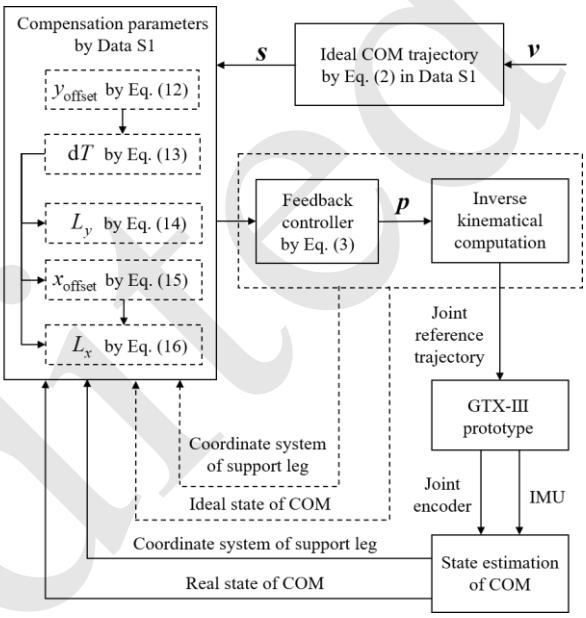

Fig. 4 Algorithm flowchart for the feedback compensation control method.

4 Simulation and Experimental Validation

As shown in Fig. 5(a), the bipedal robot considered in this study is the GTX-III prototype, with a total mass and upright COM height of 4.8 kg and 25.6 cm, respectively. Utilizing the three-dimensional simulation model of GTX-III built in Simulink (Fig. 5(b)), lateral walking, diagonal walking, and turning in place in ideal environments without disturbances or modeling errors were accomplished based on the COM trajectory-planning method proposed in Section 2. Typical lateral walking is illustrated in Fig. 6 and lateral walking experimental video screenshots are shown in Fig. 7.

Unedited

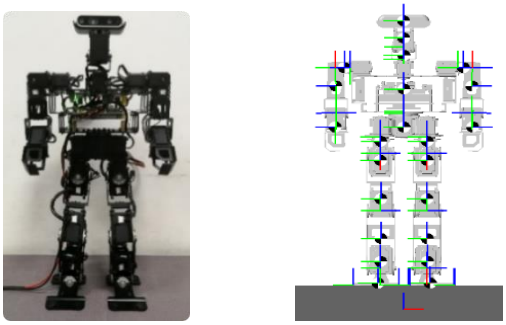

(a) Physical prototype (b) Simulink simulation model

Fig. 5 Miniature bipedal robot GTX-III.

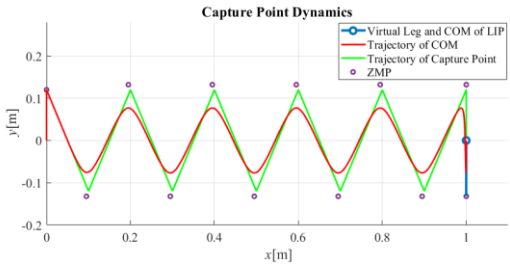

Fig. 6 Lateral walking simulation results based on the COM trajectory-planning method, with a lateral step width of 0.1 m and ideal walking cycle of 0.8 s.

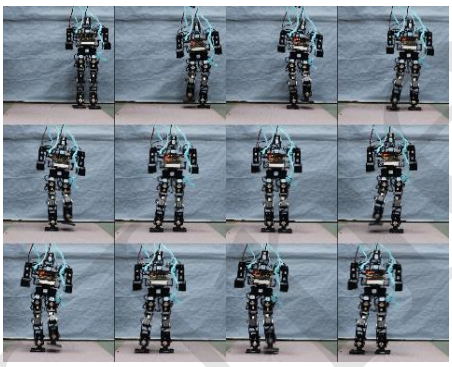

Fig. 7 Screenshots from lateral experiments based on the COM trajectory-planning method.

The following assumptions were made regarding disturbances during the robot's walking process: H1) External force disturbances were assumed to be impulse forces directly acting through the COM of the robot in three directions (generated by calling MATLAB's random number seed) with amplitudes varying within [-10, 10] N; H2). Disturbances occurred only once within a single complete gait cycle. The robot was set to walk along a straight line with an ideal support-switching interval of 0.8 s and an initial step length of 0.05 m. Simulation results are shown in Fig. 8. The randomly generated impulse force acted through the COM of the robot at the beginning of each complete gait cycle after 3 complete gait cycles, i.e., 4.8 s later. Despite the presence of external force disturbances (random impulse forces varying within [-10, 10] N), the designed disturbance-resistant control method based on bidirectional coordination promptly adjusted the foothold position to counteract the effects of external force disturbances. Although the direction of disturbance was random, similar to the characteristics of LIPM motion described in Section 2, the robot had greater freedom in forward motion. Therefore, deviations from the planned trajectory in the forward direction were smaller. However, the robot's robustness to external force disturbances was weaker in the lateral direction, necessitating adaptive adjustments in step width to accommodate external force disturbances. These adjustments allowed the COM to return to the center between the two legs through the next support switch, thus maintaining balance.

Building upon the aforementioned simulation analysis, we further conducted impact resistance tests on the bipedal robot prototype GTX-III. Screenshots from experimental videos of the disturbance-resistant walking control are shown in Fig. 8. As depicted in Fig. 9, the disturbance-resistant control strategy based on foothold-position adjustments maintained the robot's balance even in the presence of thrust disturbances. In contrast, using the COM trajectory-planning method proposed earlier resulted in imbalance under external force disturbances (omitted for brevity). Additionally, this disturbance-resistant control method effectively counteracted random external force disturbances with only a single IMU, without relying on pressure sensors on the foot sole or visual sensors. This not only provided space for subsequent multisource sensor-information fusion but also confirmed the strong robustness of the proposed disturbance-resistant control method based on foothold adjustments.

Unedited

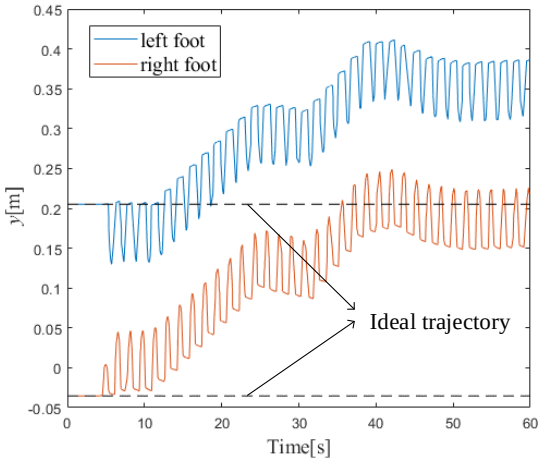

Fig. 8 Simulation results of lateral walking with resistance to random impulse disturbance based on foot placement and COM state feedback compensation.

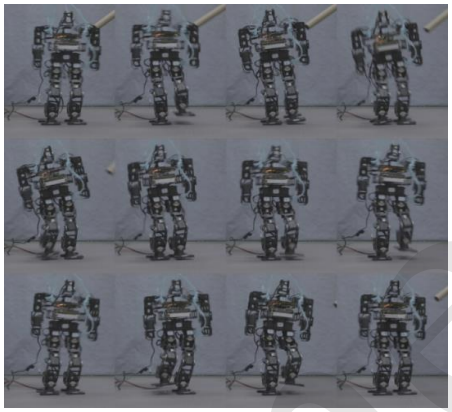

Fig. 9 Screenshots from experimental video of lateral walking with resistance to random impulse disturbance based on foot placement and COM state feedback compensation.

5 Conclusions

In this study, we first analyzed the sagittal- and coronal-plane motion during robotic walking using a LIPM, and established the CP-ZMP-COM dynamic model for it. Based on this, we propose an improved COM trajectory-planning method to achieve flexible robotic walking on flat terrain. When the robot is subjected to external force disturbances, a disturbance-resistant control strategy based on foothold and COM position adjustments can be used: when the COM reaches the support-leg swap position roughly centered in the step width, the expected touchdown time is determined by the lateral COM trajectory. By selecting appropriate lateral step widths, the COM can swing back and transition to another direction; for the highly flexible forward direction, suitable step lengths are chosen to adapt to variations in step time while maintaining the desired forward velocity; and finally, the foothold is compensated for to achieve closed-loop feedback control.

We validated the effectiveness of the COM trajectory-planning method and disturbance-resistant control strategy through experiments testing flexible walking and resistance to random impulse external force disturbances of the GTX-III prototype and its simulation model, including lateral walking, diagonal walking, and turning in place.

Acknowledgments

This work is supported by the National Natural Science Foundation of China (No. 12332023) and the Zhejiang Provincial Natural Science Foundation of China (No. LY23E050010).

Author contributions

Chunbiao GAN: Oversight and leadership responsibility for this research activity planning and execution; Zijing LI: Original draft including preparation and creation of the published work; Yimin GE: Design of methodology and application of mathematical and computational techniques; Mengyue LU: Partially process of the corresponding data.

Conflict of interest

Chunbiao GAN, Zijing LI, Yimin GE, and Mengyue LU declare that they have no conflict of interest.

References

Choi Y, Kim D, Oh Y, et al., 2007. Posture/walking control for humanoid robot based on kinematic resolution of CoM Jacobian with embedded motion. IEEE Transactions on Robotics, 23(6):1285-1293. https://doi.org/10.1109 /TRO. 2007. 904907

Englsberger J, Ott C, Roa MA, Albu-Schäffer A, Hirzinger G, 2011. Bipedal walking control based on capture point dynamics. International Conference on Intelligent Robots and Systems, 2011, p. 4420-4427.

Englsberger J, Ott C, Albu-Schäffer A, 2015. Three-dimensional bipedal walking control based on divergent component of motion. IEEE Transactions on Robotics, 31(2): 355-368. https://doi.org/10.1109/TRO.2015.2405592

Joe HM, Oh JH, 2018. Balance recovery through model predictive control based on capture point dynamics for biped walking robot. Robotics and Autonomous System, 105: 1-10. https://doi.org/ 10.1016/j.robot.2018.03.004

Jones B, Wang C, 2018. Coordinated control of centroid management and capture point for bipedal robot stability.

Unedited

International Journal of Humanoid Robotics, 41(3): 201-220. https://doi.org/ 10.1016/j.robot.2018.03.004

Kajita S, Hirukawa H, Haradra K, Yokoi K, 2014. Introduction to Humanoid Robotics. Springer Berlin Heidelberg, Germany.

Kuo AD, 2007. The six determinants of gait and the inverted pendulum analogy: A dynamic walking perspective. Human Movement Science, 26(4): 617-656. https://doi.org/10.1016/j.humov.2007. 04.003

Li THS, Kuo PH, Chen LH, Hung CC , Luan PC, Hsu HP, Chang CH, Hsieh YT, Lin WH, 2022. Fuzzy Double Deep Q-Network-Based Gait Pattern Controller for Humanoid Robots. IEEE Transactions on Fuzzy Systems, 30(1): 147-161. https://doi.org/10.1109/TFUZZ.2020. 3033141

Massah BA, Sharifi KA, Salehinia Y, Najafi F, 2012. An open loop walking on different slopes for NAO humanoid robot. International Symposium on Robotics and Intelligent Sensors, 41: 296-304. https://doi.org/10.1016/j.proeng. 2012.07.176

Park HY, Kim JH, Yamamoto K, 2022. A New Stability Framework for Trajectory Tracking Control of Biped Walking Robots. IEEE Transactions on Industrial Informatics, 18(10): 6767- 6777. https://doi.org/ 10.1109/TII.2021.3139909

Pratt J, Carff J, Drakunov S, Goswami A, 2006. Capture point: A step toward humanoid push recovery. IEEE-RAS International Conference on Humanoid Robots, p. 200-207. https://doi. org/10.1109/ichr.2006.321385

Xie H, Zhao X, Sun Q, Yang K, Li F, 2020. A new virtual-real gravity compensated inverted pendulum model and ADAMS simulation for biped robot with heterogeneous legs. Journal of Mechanical Science and Technology, 34(1): 401-412. https://doi.org/10.1007/s12206-019-1239-4

Yamamotoa K, Kamiokab T, Sugihara T, 2020. Survey on model-based biped motion control for humanoid robots. Advanced Robotics, 34 (21-22): 1353–1369. https://doi. org/10.1080/01691864.2020.1837670

Electronic supplementary materials

Data S1 Theory

中文概要

题　目：基于 CP-ZMP-COM 动力学的双足机器人质心轨迹规划及抗扰动控制

目　的：通过对成人行走过程中矢状面与冠状面内质心轨迹的分析，本文探索双足机器人自由、灵活行走的步态规划方法，并实现对其受意外外力干扰下的稳定行走。

方　法：在基于线性倒立摆模型的双足机器人运动控制中，质心、零力矩点和捕获点是实现双足机器人稳定行走的重要因素。1. 通过对矢状面与冠状面内质心运动轨迹的分析，建立双足机器人 CP-ZMP-COM 动力学模型，由此计算期望的双足机器人质心、零力矩点和捕获点，进而提出一种改进的双足机器人质心轨迹规划方法；2. 提出双足机器人在矢状面与冠状面内运动协调的抗扰动反馈补偿控制方法，对双足机器人质心和捕获点位置进行反馈补偿，使双足机器人质心和捕获点轨迹能够在后续支撑切换时逼近理想状态；3. 通过小型双足机器人样机及其仿真模型，对改进的双足机器人质心轨迹规划方法及抗扰动反馈补偿控制方法进行行走仿真与实验验证。

结　论：1. 改进的双足机器人质心轨迹规划方法可用于实现小型双足机器人横行、斜行及原地转圈等灵活行走；2. 基于所提出的抗扰动反馈补偿控制方法，小型双足机器人受随机脉冲外力下横行、斜行及原地转圈时仍能保持稳定而不摔倒。

关键词：双足机器人；CP-ZMP-COM 动力学；质心轨迹规划；反馈补偿控制

Unedited